NRC Research Press

TRIBUTE

Disulfonated xantphos for mass spectrometric mechanistic analysis

Mathias Paul, Katarina Laketic, and J. Scott McIndoe

Abstract: Xantphos is a wide bite angle bisphosphine ligand that finds wide application in catalysis. Tracking its behavior during reactions under realistic reaction conditions can be difficult at low concentrations, and although electrospray ionization mass spectrometry (ESI-MS) is effective at real-time monitoring of catalytic reactions, it can only observe ions. Accordingly, we experimented with the dianionic disulfonated version of xantphos as a charged tag for mechanistic analysis. It proved to behave exactly as hoped, providing good intensity and enabled the direct study of both an initial binding event (to copper, very fast) and a subsequent transfer to another metal (palladium). Its dianionic nature makes it especially promising for the study of reactions in which metals change charge state, because a cationic metal complex with an anionic ligand is an invisible zwitterion, whereas a dianionic ligand would instead make the same cationic complex appear due to the overall charge of −1. As such, disulfonated xantphos holds genuine promise as a mechanistic probe in real time analysis using mass spectrometry.

Key words: charge-tagged ligands, mass spectrometry, electrospray ionization, kinetics.

Résumé : Le xantphos est un ligand bisphosphine à grand angle de chélation largement employé en catalyse. Il peut être difficile de suivre son comportement dans des conditions de réaction réalistes à faibles concentrations. Bien que la spectrométrie de masse à ionisation par électronébulisation (ESIMS) soit efficace pour réaliser le suivi de réactions catalytiques en temps réel, elle ne permet d'observer que des ions. Nous avons donc réalisé des expériences à des fins d'analyse mécanistiques avec la version dianionique disulfonée du xantphos comme ligand marqué par charge. Le ligand marqué s'est comporté exactement comme nous l'avions escompté : donnant lieu à un signal de bonne intensité, il a permis l'observation directe de l'étape de liaison initiale (au cuivre, très rapide) et du transfert subséquent à un autre métal (le palladium). Par sa nature dianionique, il constitue une avenue fort prometteuse pour l'étude des réactions dans lesquelles les métaux changent d'état de charge, étant donné qu'un complexe de métal cationique avec un ligand anionique forme un zwitterion invisible, contrairement à un ligand dianionique, qui permet de rendre le même complexe cationique visible grâce à une charge globale de −1. Dans ce contexte, les xantaphos disulfonés se révèlent être réellement prometteurs comme sondes pour réaliser des analyses mécanistiques en temps réel à l'aide de la spectrométrie de masse. [Traduit par la Rédaction]

Mots-clés : ligands marqués par charge, spectrométrie de masse, ionisation par électronébulisation, cinétique.

Introduction

Catalytic systems are tough to study directly. Even in homogeneous systems, the solution is a complex mixture of solvent, reactants, products, and byproducts.[1–5] Catalytically relevant species are typically much less abundant than the aforementioned and partitioned between precatalyst, resting state(s), decomposition products, and intermediates, and only a fraction may be on-cycle at any point in time.[6–15] Direct methods of investigation need to be sufficiently sensitive to delve down to very low concentration levels, and in electrospray ionization mass spectrometry (ESI-MS), chemists have a tool to do exactly that. However, the technique has an Achilles heel: it operates solely on ions, transferring them to the gas phase for analysis, and ignores neutral compounds, which are unaffected by the electric fields used to manipulate charged species. Chemists wishing to probe catalytic reactions by ESI-MS need to either limit themselves to ionic catalysts or come up with ways to tag otherwise neutral compounds with a charge to render them visible.[16–24] Here, we have adopted the disulfonated version of the popular wide bite angle ligand xantphos,[25–28] and examined its potential as a charged-tagged ligand for mechanistic analysis.[29]

We chose to examine the coordination of disulfonated xantphos to copper(I) iodide, as this ligand/metal combination has been used with success in various catalytic transformations but the ligand is also widespread in other transformations.[25,30–35] We were particularly interested in the report[34] that a co-catalytic system for direct arylation of heteroarenes involved a xantphos complex of copper that did not exchange ligands with the palladium present (Schemes 1 and 2). Given that xantphos typically enthusiastically binds Pd,[36–38] we planned to probe the copper/palladium/xantphos interaction in more detail using real-time ESI-MS,[39,40] as a way to assess its efficacy as a reaction probe and to point the way to further mechanistic studies.

As can be seen in Scheme 1, Huang and coworkers interpret the catalytic direct arylation of heteroarenes as follows. In a first cycle, the preformed copper-xantphos complex **I** coordinates the benzothiazole first to from the *N*-coordinated species **II** and

Received 13 August 2020. Accepted 13 October 2020.

M. Paul, K. Laketic, and J.S. McIndoe. Department of Chemistry, University of Victoria, P.O. Box 1700 STN CSC, Victoria, BC V8W 2Y2, Canada.

Corresponding author: J. Scott McIndoe (email: mcindoe@uvic.ca).

This paper is part of a special issue to honor Professor Robert H. Morris.

Scheme 1. Mechanistic interpretation as proposed by Huang and coworkers.[34,41] [Colour online.]

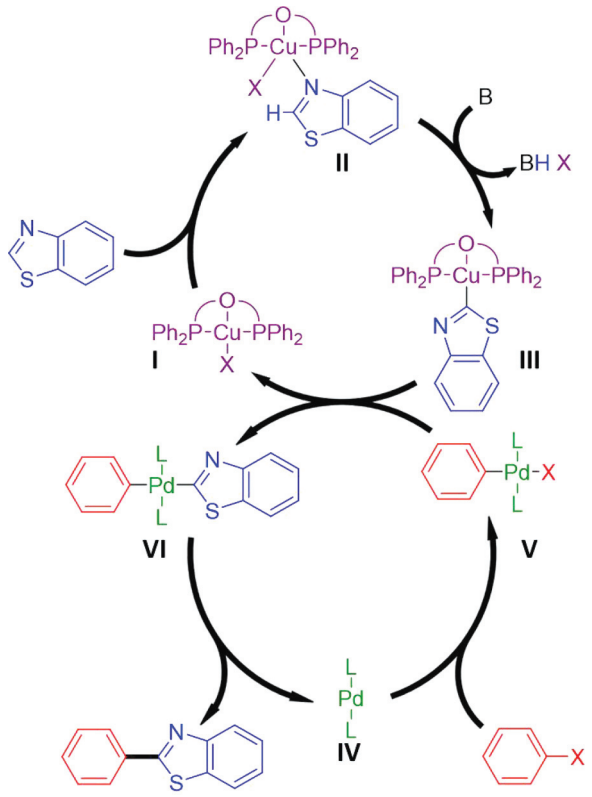

deprotonation yields carbene complex **III**. In a second cycle, a palladium(0) catalyst **IV** undergoes oxidative addition with a phenyl halide to form the palladium(II) intermediate **V**. Through transmetallation, the benzothiazole is transferred to the palladium center, regenerating the copper cocatalyst **I** and generating the palladium(II) species **VI**. In the final step of these Pd/Cu double-cocatalytic cycles, the arylated product is formed through reductive elimination, regenerating the active palladium(0) catalyst. At no point in their study was Pd/Cu crossover reaction on the xantphos ligand observed.[34]

Results and discussion

Disulfonated xantphos was synthesized following a procedure derived from the one used by van Leeuwen and coworkers (Scheme 2).[27] To make the ligand more soluble in organic solvents, we replaced the sodium counterions with hydrophobic bis (triphenylphosphine)iminium cations ([PPN]$^+$). We characterized the sodiated sulfonated xantphos dianion, henceforth [**1**]$^{2-}$, mass spectrometrically in negative ion mode. It provided a strong signal at *m*/*z* 368, with an isotope pattern commensurate with a dianionic formulation (peaks in the pattern *m*/*z* 0.5 apart, see Fig. 1). The spectrum looks more complicated than expected for a clean compound, but combinations of the dianion and the sodium cation and trace oxidation readily account for nearly all species.[42] The exception is a small amount of triply sulfonated xantphos at *m*/*z* 272.

To examine the reactivity of ions using ESI-MS, we employ pressurized sample infusion (PSI) to monitor the reactions continuously in real-time.[43] PSI is essentially a cannula transfer using a capillary, which generates flow rates suitable for ESI-MS analysis.[44] When we examined the reaction between CuI and PPN_2[**1**] in acetonitrile at room temperature (Fig. 2), we were surprised to see that ligand association happened faster than the timescale of the PSI-ESI-MS experiment (which requires 10 s for the solution to be pumped from the reaction flask to the mass spectrometer).[45]

As the main product, a dianionic complex whose mass spectrometric profile corresponded to [Cu(**1**)I]$^{2-}$ in terms of *m*/*z*, isotope pattern, and MS/MS behavior (Fig. 3). It is reasonable to assume rapid association reaction happens because of the chelate effect of the bidentate [**1**]$^{2-}$, which can therefore abstract copper from the tetrakis(acetonitrile)copper(I) complex. A substantial amount of $[CuI_2]^-$ was also observed, with concomitant formation of $[Cu(NCMe)_n]^+$ (n = 2–4) in the positive ion mode.

As seen in Fig. 3, [Cu(**1**)I]$^{2-}$ at *m*/*z* 463 undergoes unimolecular decomposition in the gas-phase primarily by loss of I$^-$ (*m*/*z* 127) to generate [Cu(**1**)]$^-$, *m*/*z* 799. A small amount of oxygen atom loss from this ion is also observed (*m*/*z* 783).

The straightforward production of [Cu(**1**)I]$^{2-}$ in solution provided an opportunity to assess the relative propensity of binding of the disulfonated xantphos [**1**]$^{2-}$ for Cu(I) vs. Pd(0). At 35 °C, this reaction is fast ($t_{1/2} \sim 1$ min) and complete, with [**1**]$^{2-}$ abandoning Cu(I) entirely and taking up residence on Pd(0) (Fig. 4). An equilibrium is established in which we observe both [Pd(**1**)(dba)]$^{2-}$ (*m*/*z* 538) and [Pd(**1**)$(dba)_2$]$^{2-}$ (*m*/*z* 655) in an approximately 4:1 ratio.

Both of these palladium(0) species readily lose a dba ligand in the gas phase when subjected to collision-induced dissociation (Fig. 5). The coordination of the [Pd(**1**)$(dba)_2$]$^{2-}$ is not provided by ESI-MS, but the presence of three bidentate ligands means a variety of possibilities depending on binding modes.

The published observation that xantphos does not transfer from Cu(I) to Pd(0) under catalytic conditions probably has several contributing factors. Toluene (the solvent used) is non-polar and minimally capable of mediating the ligand exchange, unlike the polar solvents used in this study. Acetonitrile is good at coordinating to both copper and palladium and thus can stabilize the unsaturated intermediates required for xantphos to migrate from one metal to the other. Also, the palladium center in that case had a much more robust ligand set (P^tBu_2Cl) rather than the weakly coordinating dibenzylideneacetone or acetonitrile ligand. Furthermore, the difference between the non-sulfonated and sulfonated xantphos ([**1**]$^{2-}$) as a ligand could certainly contribute to the differences seen.

Experimental

All synthetic operations and catalyst preparations were carried out under a nitrogen (N_2) atmosphere, using Schlenk techniques and a glovebox.

Mass spectrometry was performed on a Waters Acquity Triple Quadrupole Detector (TQD). NMR spectra were recorded at room temperature using a Bruker Avance-III 300 NMR using either methanol-d_4 or acetonitrile-d_3 as the solvent. Chemicals were purchased from Sigma Aldrich and used as received.

Synthesis of 2,7-bis(SO_3Na)-xantphos Na_2[1]

The method was adapted from van Leeuwen and coworkers.[28] Under a stream of nitrogen, xantphos (1.00 g, 1.73 mmol) was carefully added to oleum (2.9 mL, 25% SO_3) at 5 °C over the course of 4 h. Upon addition, the resulting light brown solution was warmed to room temperature and stirred for 12 h. After that, degassed water (15 mL) was added slowly to the solution, which resulted in a white suspension. Further degassed water (20 mL) was added at once, and the resulting yellow solution was then poured into a vigorously stirred solution of triisooctylamine (54 mmol, 2.3 mL in 10 mL of toluene). The toluene layer was washed twice with water before careful adjustment of the pH to 12 using NaOH solution (6.25 mol/L). The water layer was decanted and neutralized with H_2SO_4 (3.00 mol/L). Evaporation gave a white solid, which was suspended in refluxing methanol and filtered hot. The filter cake was washed a couple of times with further hot methanol and the resulting filtrate evaporated to dryness. Further purification was done by refluxing the solid in

Scheme 2. Synthesis of the sodium salt of sulfonated xantphos by a procedure derived from the one used by van Leeuwen and coworkers,[27] followed by ion exchange.

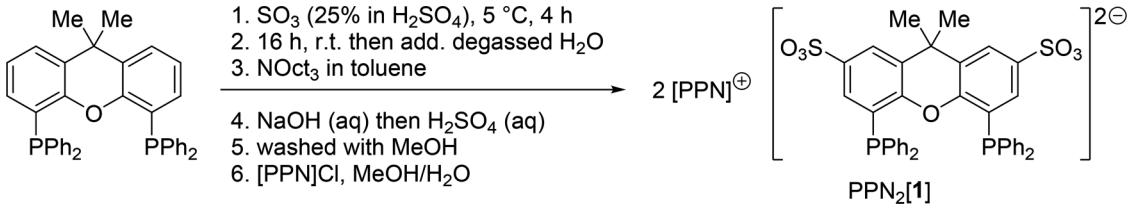

Fig. 1. Negative ion mass spectrum of crude $[\mathbf{1}]^{2-}$ in acetonitrile. The inset shows the isotope pattern. The internal standard (IS) is $[B(C_6F_5)_4]^-$. [Colour online.]

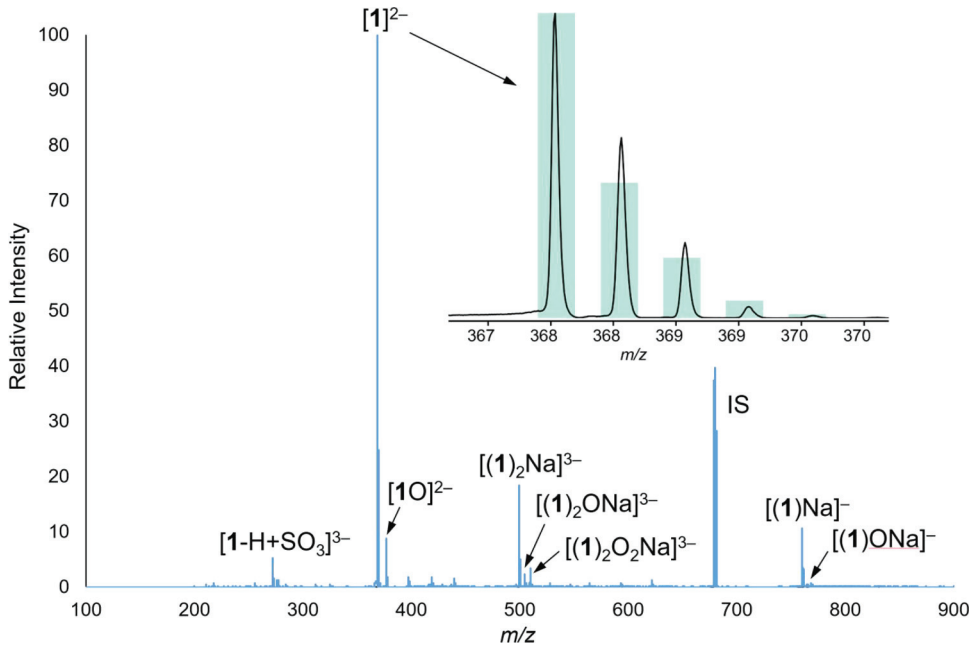

Fig. 2. Reaction profile for the combination of $[PPN]_2[\mathbf{1}]$ and CuI in acetonitrile. Intensities are normalized to the total ion current of the species shown. [Colour online.]

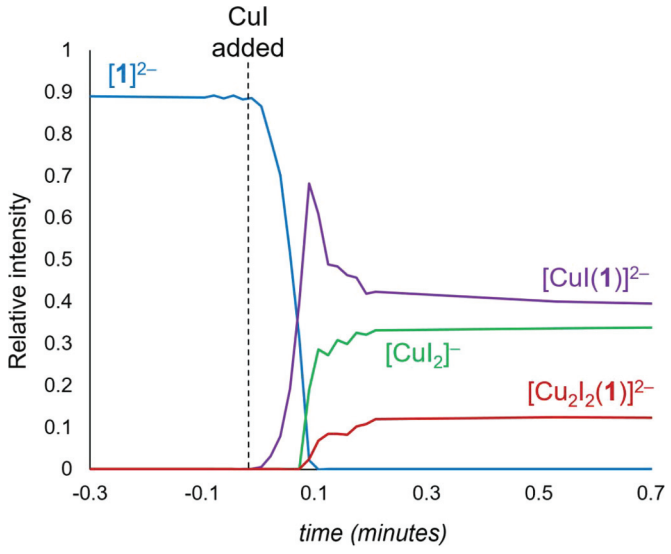

EtOH, which yielded a white solid. Yield: 1.10 g, 1.41 mmol, 82%. ^{1}H NMR (300 MHz CD_3OD, 298 K) δ [ppm] = 8.00 (d, J = 2.0 Hz, 2H), 7.30 – 7.23 (m, 12H), 7.21 – 7.13 (m, 10H), 1.69 (s, 6H). ^{31}P NMR (122 MHz CD_3OD, 298 K) δ [ppm] = –17.62 (s, 2 P). ESI-MS (–ve): m/z 368.05 $[C_{39}H_{30}O_7P_2S_2]^{2-}$.

Synthesis of 2,7-bis(SO_3PPN)-xantphos $[PPN]_2[\mathbf{1}]$

A round-bottomed flask equipped with a stir bar was charged with the sodium salt of sulfonated xantphos ($Na_2[\mathbf{1}]$) (0.507 g, 0.644 mmol, 1.00 eq) and PPNCl (0.739 g, 1.288 mmol, 2.00 eq). It was dissolved in as little methanol as possible (approximately 4 mL). An equal amount of water was added, and the slightly cloudy mixture heated until it was clear again. This solution was placed in a fridge at 5 °C for 3 days. The desired product precipitated as a colourless powder and was collected using vacuum filtration. It was washed using a cold methanol/water mixture (1:1) and dried under reduced pressure. Yield: 1.05 g, 0.579 mmol, 90%. ^{1}H NMR (300 MHz CD_3CN, 298 K) δ [ppm] = 7.84 (d, J = 2.0 Hz, 2H), 7.69 – 7.52 (m, 36H), 7.50 – 7.42 (m, 24H), 7.33 – 7.25 (m, 12H), 7.19 – 7.09 (m, 8H), 6.92 (psq, 2H) 1.56 (s, 6H). ^{31}P NMR (122 MHz CD_3CN, 298 K) δ [ppm] = 20.75 (s, 4 P), –17.88 (s, 2 P). ESI-MS: (+ve) m/z 538.6 $[C_{36}H_{30}NP_2]^+$; (–ve) m/z 368.0 $[C_{39}H_{30}O_7P_2S_2]^{2-}$.

Synthesis of copper complex $[PPN]_2[Cu(1)I]$

A round-bottomed flask equipped with a stir bar was charged with $[PPN]_2[\mathbf{1}]$ (0.100 g, 0.504 mmol, 1.00 eq) and copper(I) iodide (0.096 mg, 0.504 mmol, 1.00 eq). To this acetonitrile (10.0 mL) was added and the flask sealed with a septum. The prepared flask was

Fig. 3. Negative ion product ion mass spectrum of $[Cu(\mathbf{1})I]^{2-}$. The inset shows the isotope pattern (line) shown with simulated pattern (bars). [Colour online.]

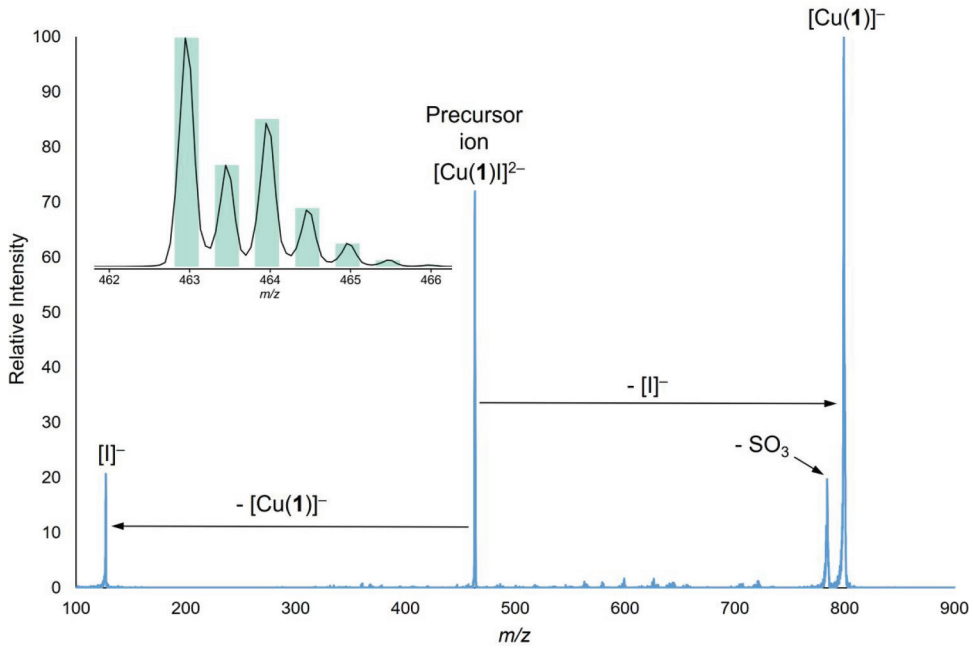

Fig. 4. Reaction profile for the combination of $[Cu(\mathbf{1})I]^{2-}$ and $Pd_2(dba)_3$ in acetonitrile. Intensities are normalized to the sum of all species containing $[\mathbf{1}]^{2-}$. The proposed structure for $[Pd(\mathbf{1})(dba)]^{2-}$ is based on a crystal structure of the non-sulfonated derivative reported by Macgregor, Grushin, and coworkers.[46] A similar structure was observed by Buchwald and coworkers for 4,7-di-*tert*-butyl xantphos using NMR.[47] [Colour online.]

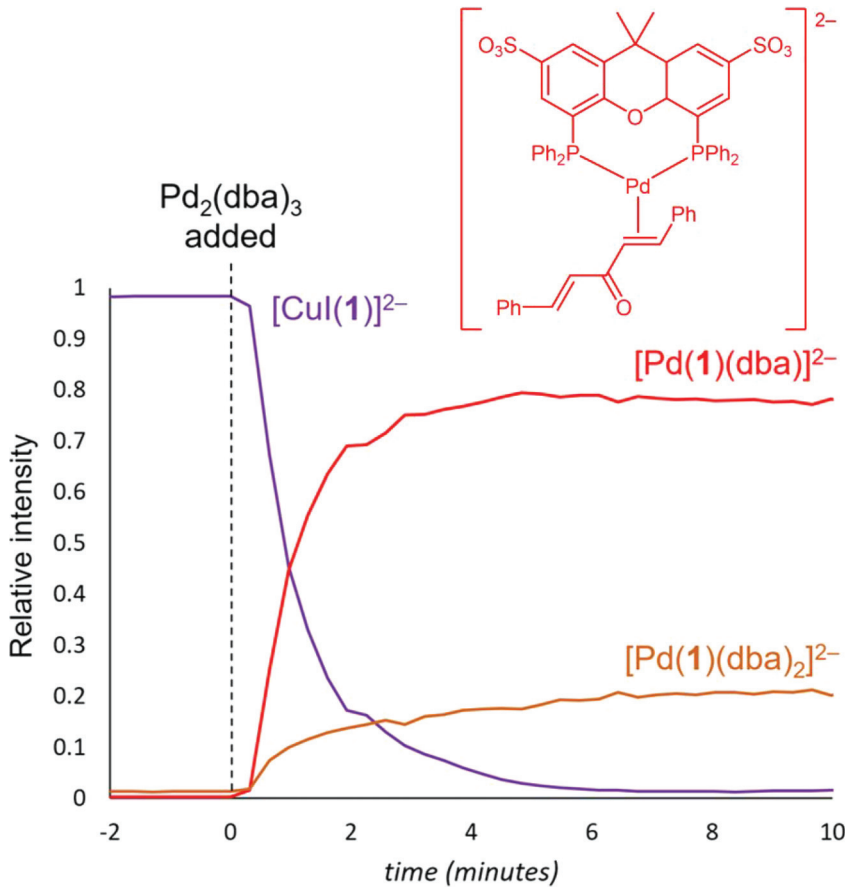

Fig. 5. Negative ion product ion ESI mass spectrum of $[Pd(\mathbf{1})(dba)]^{2-}$. The inset shows the isotope pattern shown with simulated pattern. [Colour online.]

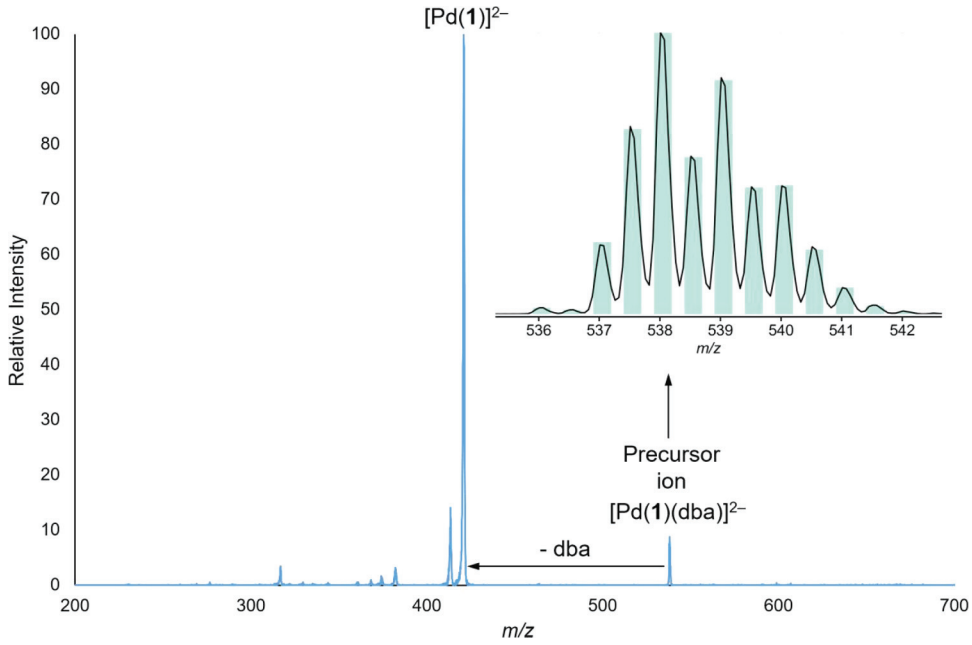

placed in an oil bath and stirred at 80 °C for 15 h. After the clear solution had cooled to room temperature, the volatiles were removed under reduced pressure to leave the product as a colourless powder. ^{1}H NMR (300 MHz CD_3CN, 298 K) δ [ppm] = 7.95 (brd, J = 2.0 Hz, 2H), 7.68 – 7.53 (m, 36H), 7.51 – 7.42 (m, 32H) 7.31 (brt, J = 7.2 Hz, 4H), 7.22 (brt, J = 7.2 Hz, 8H), 7.00 (m, 2H), 1.54 (s, 6H). ^{31}P NMR (122 MHz CD_3CN, 298 K) δ [ppm] = 20.76 (s, 4 P), −20.53 (brs, 2 P). ESI-MS: (+ve) m/z 538.6 $[C_{36}H_{30}NP_2]^+$; (–ve): m/z 463.0 $[C_{39}H_{30}CuIO_7P_2S_2]^{2-}$.

In situ synthesis of palladium complexes

In a glovebox, $[PPN]_2[Cu(\mathbf{1})I]$ (10.8 mg, 5.4 μmol) was placed in a Schlenk flask with dry acetonitrile (10.0 mL). $Pd_2(dba)_3$ (5.0 mg, 5.5 μmol) was placed in a round-bottomed flask with dry CH_3CN (5.5 mL) and appeared as a black solution. The copper complex was initially monitored via mass spectrometry in negative ion mode under argon gas, and then, the $Pd_2(dba)_3$ solution was added at once to the copper complex solution and monitoring continued for any changes.

Conclusions

The efficacy of disulfonated xantphos, $PPN_2[\mathbf{1}]$, as a mechanistic probe in ESI-MS studies has been demonstrated in preliminary experiments. Dianionic ligands have a downside in that they have considerably different solubility profiles than their neutral analogues. However, they have double upsides in the context of ESI-MS-based mechanistic analysis: they not only render neutral complexes visible, but also can cope with changes in charge state during reactions. This property was evident indirectly in this study, because although both CuI and Pd(dba) are neutral fragments, we were also able to observe the monoanionic complex $[Cu\mathbf{1}]^-$ that initially formed when $[\mathbf{1}]^{2-}$ reacted with Cu^+. We anticipate this capability being useful in cases not just involving xantphos, but for any ligand that can be multiply charged through sulfonation (or other means), because instead of a cationic signal disappearing due to zwitterion formation, it will simply convert to a monoanion instead and remain trackable by ESI-MS. As such, $[\mathbf{1}]^{2-}$ promises to be a useful addition to the arsenal of mechanistic probes for the study of complex catalytic transformations.

Supplementary data

Supplementary data are available with the article at https://doi.org/10.1139/cjc-2020-0350.

Acknowledgements

JSM thanks the NSERC Discovery program for operational funding and CFI, BCKDF, and the University of Victoria for infrastructural support. KL thanks the University of Victoria for a Jamie Cassels Undergraduate Research Award and NSERC for an Undergraduate Summer Research Award. Anuj Joshi is thanked for running ^{1}H and ^{31}P NMR experiments. Rina Concepcion and Dr. Antonio Eduardo Miller Crotti are thanked for assistance with some experiments.

References

(1) Malig, T. C.; Yu, D. N.; Hein, J. E. *J. Am. Chem. Soc.* **2018**, *140* (29), 9167. doi:10.1021/jacs.8b04635.
(2) Isbrandt, E. S.; Sullivan, R. J.; Newman, S. G. *Angew. Chem. Int. Ed.* **2019**, *58* (22), 7180. doi:10.1002/anie.201812534.
(3) Christensen, M.; Adedeji, F.; Grosser, S.; Zawatzky, K.; Ji, Y. N.; Liu, J. C.; Jurica, J. A.; Naber, J. R.; Hein, J. E. *React. Chem. Eng.* **2019**, *4* (9), 1555. doi:10.1039/C9RE00086K.
(4) van Leeuwen, P. W. N. M. Homogeneous Catalysis – Understanding the Art. 1 ed.; Kluwer Academic Publishers, Dordrecht, Boston, London: Netherlands 2004.
(5) Behr, A. and Neubert, P. Applied Homogeneous Catalysis. First ed.; Wiley VCH: Weinheim, Germany 2012.
(6) Selent, D. and Heller, D. Catalysis: From Principles to Applications. Wiley VCH: Weinheim, Germany 2012.
(7) Yarwood, J., Douthwaite, R., and Duckett, S. B. Spectroscopic Properties of Inorganic and Organometallic Compounds. RSC Publishing: Cambridge 2010.
(8) Hartwig, J. F. Organotransition Metal Chemistry: From Bonding to Catalysis. University Science Books, VA 2009.
(9) Jordan, R. B. Reaction Mechanisms of Inorganic and Organometallic Systems. Third ed.; Oxford University Press: New York, NY, USA 2007.
(10) Bligaard, T.; Bullock, R. M.; Campbell, C. T.; Chen, J. G. G.; Gates, B. C.; Gorte, R. J.; Jones, C. W.; Jones, W. D.; Kitchin, J. R.; Scott, S. L. *ACS Catal.* **2016**, *6* (4), 2590. doi:10.1021/acscatal.6b00183.

(11) Xu, Q. S.; Guo, L. F.; Dinh, T. N.; Cheong, A.; Garland, M. *ACS Catal.* **2015**, *5* (6), 3588. doi:10.1021/cs502127y.
(12) Blackmond, D. G. *J. Am. Chem. Soc.* **2015**, *137* (34), 10852. doi:10.1021/jacs.5b05841.
(13) Grabow, K.; Bentrup, U. *ACS Catal.* **2014**, *4* (7), 2153. doi:10.1021/cs500363n.
(14) Torres, A.; Perez, N. M.; Overend, G.; Hodge, N.; Heaton, B. T.; Iggo, J. A.; Satherley, J.; Whyman, R.; Eastham, G. R.; Gobby, D. *ACS Catal.* **2012**, *2* (11), 2281. doi:10.1021/cs300439n.
(15) Garland, M.; Li, C. Z.; Guo, L. F. *ACS Catal.* **2012**, *2* (11), 2327. doi:10.1021/cs3004209.
(16) Iacobucci, C.; Reale, S.; De Angelis, F. *Angew. Chem. Int. Ed.* **2016**, *55* (9), 2980. doi:10.1002/anie.201507088.
(17) Iacobucci, C.; Reale, S.; Gal, J. F.; De Angelis, F. *Angew. Chem. Int. Ed.* **2015**, *54* (10), 3065. doi:10.1002/anie.201410301.
(18) Medeiros, G. A.; da Silva, W. A.; Bataglion, G. A.; Ferreira, D. A. C.; de Oliveira, H. C. B.; Eberlin, M. N.; Neto, B. A. D. *Chem. Commun.* **2014**, *50* (3), 338. doi:10.1039/C3CC47156J.
(19) Iacobucci, C.; Reale, S.; Gal, J. F.; De Angelis, F. *Eur. J. Org. Chem.* **2014**, *2014* (32), 7087. doi:10.1002/ejoc.201403179.
(20) Coelho, F.; Eberlin, M. N. *Angew. Chem. Int. Ed.* **2011**, *50* (23), 5261. doi:10.1002/anie.201008082.
(21) Marquez, C. A.; Fabbretti, F.; Metzger, J. O. *Angew. Chem. Int. Ed.* **2007**, *46* (36), 6915. doi:10.1002/anie.200700266.
(22) Meyer, S.; Koch, R.; Metzger, J. O. *Angew. Chem. Int. Ed.* **2003**, *42* (38), 4700. doi:10.1002/anie.200352044.
(23) Adlhart, C.; Chen, P. *HCA.* **2000**, *83* (9), 2192. doi:10.1002/1522-2675(20000906)83:9<2192::AID-HLCA2192>3.0.CO;2-G.
(24) Hinderling, C.; Adlhart, C.; Chen, P. *Angew. Chem. Int. Ed.* **1998**, *37* (19), 2685. doi:10.1002/(SICI)1521-3773(19981016)37:19<2685::AID-ANIE2685>3.0.CO;2-M.
(25) van Leeuwen, P. W. N. M.; Kamer, P. C. J. *Catal. Sci. Technol.* **2018**, *8* (1), 26. doi:10.1039/C7CY01629H.
(26) Hanson, B. E. *Coord. Chem. Rev.* **1999**, *185-6*, 795.
(27) Goedheijt, M. S.; Reek, J. N. H.; Kamer, P. C. J.; van Leeuwen, P. W. N. M. *Chem. Commun.* **1998**, (22), 2431. doi:10.1039/a806446f.
(28) Goedheijt, M. S.; Kamer, P. C. J.; van Leeuwen, P. W. N. M. *J. Mol. Catal. A: Chem.* **1998**, *134* (1–3), 243.
(29) Chisholm, D. M.; McIndoe, J. S. *Dalton Trans.* **2008**, (30), 3933. doi:10.1039/b800371h.
(30) Takahashi, R.; Kubota, K.; Ito, H. *Chem. Commun.* **2020**, *56* (3), 407. doi:10.1039/C9CC06946A.
(31) Viciano-Chumillas, M.; Carbonell-Vilar, J. M.; Armentano, D.; Cano, J. *Eur. J. Inorg. Chem.* **2019**, *2019* (25), 2982. doi:10.1002/ejic.201900323.
(32) Adams, G. M.; Colebatch, A. L.; Skornia, J. T.; McKay, A. I.; Johnson, H. C.; Lloyd-Jones, G. C.; Macgregor, S. A.; Beattie, N. A.; Weller, A. S. *J. Am. Chem. Soc.* **2018**, *140* (4), 1481. doi:10.1021/jacs.7b11975.
(33) Liu, M. L.; Ye, M. Y.; Xue, Y. Y.; Yin, G. D.; Wang, D. J.; Huang, J. K. *Tetrahedron Lett.* **2016**, *57* (29), 3137. doi:10.1016/j.tetlet.2016.06.014.
(34) Huang, J. K.; Chan, J.; Chen, Y.; Borths, C. J.; Baucom, K. D.; Larsen, R. D.; Faul, M. M. *J. Am. Chem. Soc.* **2010**, *132* (11), 3674. doi:10.1021/ja100354j.
(35) Marchetti, M.; Botteghi, C.; Paganelli, S.; Taddei, M. *Adv. Synth. Catal.* **2003**, *345* (11), 1229. doi:10.1002/adsc.200303053.
(36) Seomoon, D.; Lee, P. H. *J. Org. Chem.* **2008**, *73* (3), 1165. doi:10.1021/jo702279t.
(37) Yin, J. J.; Buchwald, S. L. *J. Am. Chem. Soc.* **2002**, *124* (21), 6043. doi:10.1021/ja012610k.
(38) Artamkina, G. A.; Sergeev, A. G.; Beletskaya, I. P. *Tetrahedron Lett.* **2001**, *42* (26), 4381. doi:10.1016/S0040-4039(01)00716-X.
(39) Yunker, L. P. E.; Ahmadi, Z.; Logan, J. R.; Wu, W. Z.; Li, T. F.; Martindale, A.; Oliver, A. G.; McIndoe, J. S. *Organometallics.* **2018**, *37* (22), 4297. doi:10.1021/acs.organomet.8b00705.
(40) Janusson, E.; Zijlstra, H. S.; Nguyen, P. P. T.; MacGillivray, L.; Martelino, J.; McIndoe, J. S. *Chem. Commun.* **2017**, *53* (5), 854. doi:10.1039/C6CC08824D.
(41) McFarlane, J.; Henderson, B.; Donnecke, S.; McIndoe, J. S. *Organometallics.* **2019**, *38* (21), 4051. Scheme drawn using, www.catacycle.com. doi:10.1021/acs.organomet.9b00563.
(42) McIndoe, J. S.; Vikse, K. L. *J. Mass Spectrom.* **2019**, *54* (5), 466. doi:10.1002/jms.4359.
(43) Vikse, K. L.; Ahmadi, Z.; Luo, J. W.; van der Wal, N.; Daze, K.; Taylor, N.; McIndoe, J. S. *Int. J. Mass Spectrom.* **2012**, *323*, 8.
(44) Yunker, L. P. E.; Stoddard, R. L.; McIndoe, J. S. *J. Mass Spectrom.* **2014**, *49* (1), 1. doi:10.1002/jms.3303.
(45) Ray, A.; Bristow, T.; Whitmore, C.; Mosely, J. *Mass Spec. Rev.* **2018**, *37* (4), 565. doi:10.1002/mas.21539.
(46) Miloserdov, F. M.; McMullin, C. L.; Belmonte, M. M.; Benet-Buchholz, J.; Bakhmutov, V. I.; Macgregor, S. A.; Grushin, V. V. *Organometallics.* **2014**, *33* (3), 736. doi:10.1021/om401126m.
(47) Klingensmith, L. M.; Strieter, E. R.; Barder, T. E.; Buchwald, S. L. *Organometallics.* **2006**, *25* (1), 82. doi:10.1021/om050715g.